Available online **www.ijpras.com**

International Journal of Pharmaceutical Research & Allied Sciences, 2016, 5(2):93-102

Research Article

ISSN : 2277-3657
CODEN(USA) : IJPRPM

Design, Molecular Docking and Pharmacokinetic Study of Novel Isatin Derivatives as Anti-HIV Agents

Neeraj Kumar[1], Shashank Shekhar Mishra[2], Chandra Shekhar Sharma[2], Hemendra Pratap Singh[2] and Sourav Kalra[3]

[1]Department of Pharmaceutical Chemistry, Geetanjali Institute of Pharmacy, Udaipur 313001, India
[2]Department of Pharmaceutical Chemistry, B. N. College of Pharmacy, Udaipur 313001, India
[3]Central University of Punjab, Bhatinda

ABSTRACT

Isatin analogues have versatile biological activities due to the presence of indole backbone. Today, AIDS is one of the most challenging and escalating health problems and NNRTIs are commonly used drugs for the treatment. The aim of this work is to design novel isatin derivatives as more potent and effective anti-HIV agents. Molecular docking studies were performed for the title compounds on six different high resolution crystal structure of the Reverse Transcriptase (RT) enzyme with five drugs Efavirenz, Etravirine, Delaviridine, Nevirapine, and Rilpivirine. Pharmacokinetic properties and drug-likeness of the title compounds were also analyzed by using QuikProp. Combined G Score of compound S5 (-58.6) was comparable with standard drugs, suggested that designed isatin derivatives have a good binding affinity for HIV-1 RT enzyme. Pharmacological study results indicated that all designed compounds have a promising pharmacological profile and drug-likeness property.

Keywords: NNRTIs, Isatin, HIV, Reverse Transcriptase (RT)

INTRODUCTION

Viral diseases are highly contagious and escalating health problems that reached epidemic proportions in all countries of the world with a large increase in economic burden with mortality. But effective and early pharmacotherapy is curable to control and prevent the diseases.

Acquired Immunodeficiency Syndrome (AIDS) is a lethal disorder caused by Human Immunodeficiency Virus (HIV) and exists under two forms: HIV-1 and HIV-2, in which the mortality rate is high for HIV-1. At present, there is no vaccine available for HIV treatment. Currently, HIV infection is prevented by the prominent use of anti-viral drugs that belongs to the category of HIV protease inhibitors, entry inhibitors, chemokine receptor binders,integrase inhibitors, nucleoside/nucleotide reverse transcriptase inhibitors (NRTIs/NTRIs) and non-nucleoside reverse transcriptase inhibitors (NNRTIs)[1].

NRTIs inhibits are highly selective and non-competitive inhibitors of HIV-1 reverse transcriptase. NRTIs bind to reverse transcriptase (RT) at a adjacent site to the active site (Non-nucleoside binding pocket-NNBP), inducing a conformational change that results in inhibition of enzyme with the lack of cross-resistance [2]. So, reverse transcriptase is one of the most promising targets for the design of effective anti-HIV drug. At present, NNRTIs (Fig. 1) used for treatment of AIDS are Delaviridine (DLV), Efavirenz (EFV), Etravirine (ETV), Nevirapine (NVP) and Rilpivirine (RPV).

Isatin derivatives possess pharmacological activities such as antiviral, anti-HIV, antibacterial, antifungal, anticonvulsant activity, anti-inflammatory and analgesic activity [3-8]. Due to indole nucleus and having wide spectrum chemotherapeutic properties, isatin is a biologically validated pharmacophore for the design and development new chemical entities. In context with previous rationale and focusing on searching novel structural leads with potential anti-HIV activity, substituted isatin derivatives have been designed.

In the present study, some novel isatin derivatives were designed and the binding mode was investigated by docking studies with six different structures of HIV-1 RT enzyme (PDB Codes: 1REV, 1SV5, 1IKY, 1KLM, 1IKW and 1TKZ) complexed with five different ligands Delaviridine, Efavirenz, Etravirine, Nevirapine and Rilpivirine. Furthermore, all designed compounds were subjected to pharmacokinetic study and drug likeness.

In this work, we have concentrated on optimization of pharmacophore by understanding different binding interactions of novel isatin derivatives by using molecular docking studies. In designing an effective anti-viral drug against HIV, the type and number of binding interactions present in amino acid residue were also studied for finding the structural requirements for designing an effective anti-HIV drug.

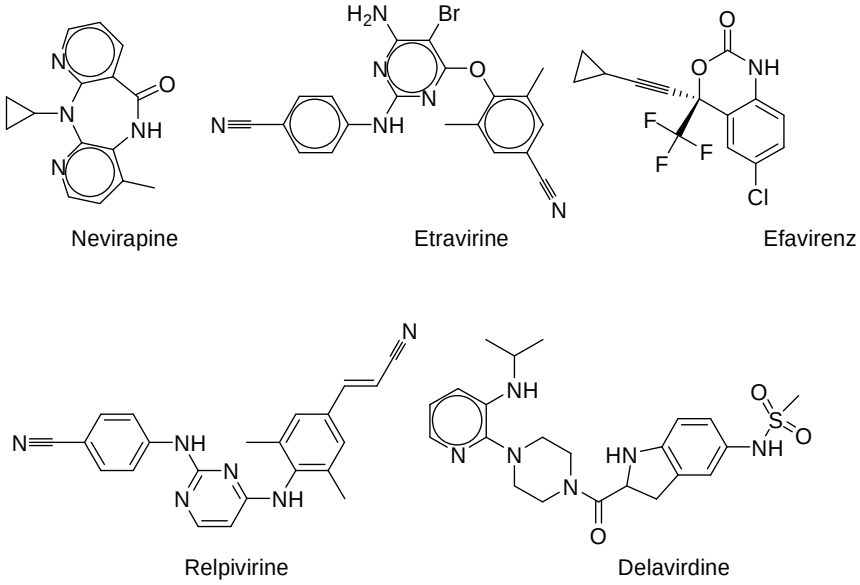

Fig. 1 Structure of currently used NNRTIs

MATERIALS AND METHODS

Ligand preparation

Designed compounds have appropriate bond order and in 2D structure which were converted into maestro format. All structures were optimized by use of MMFF94 force field and generated possible ionisation states in the target pH range 7.0±2 by using epic default settings [9] using LigPrep 2.3 application (Schrödinger).

Selection of protein structures

The six crystal protein structures of HIV-1 reverse transcriptase were obtained from the RCSB protein data bank. These structures of HIV-1 RT were 1KLM, 1REV, 1SV5, 1TKZ, 1IKY and 1IKW. 1KLM and 1REV are categorised under nucleonics transferase, and four 1SV5, 1TKZ, 1IKY and 1IKW are categorised under transferase.

Protein preparation

A PDB crystal structure consists of water molecules, heavy atoms, metal ions and cofactors. Schrödinger developed a set of tools that prepare a protein structure in the acceptable format for modelling experiments. Since Glide docking experiments utilize only single protein geometry, all structures were reduced to a single unit. PDB structures also have missing information on molecular topologies, formal charge and assigned bond order. Commonly, X-ray structure analysis does not recognize NH_2 and O that results misaligned terminal amide groups. Glide calculation needs ionization states and bond orders to be properly allocated and performed more effectively when side chains are reoriented, to relieve essential and steric clashes.

All protein structures were prepared for molecular docking using the “protein preparation wizard”. All the water molecules in PDB structure were deleted and Hydrogen’s were added. Preparation of protein structure associated on two steps, preparation of protein and refinement of protein. In the preparation of protein, after preprocess,

protonation and metal charge states were generated. A single co-crystallized protein structure was selected for docking. Hydrogen bonds were optimized by water molecules, reorienting hydroxyl groups, and amide groups of Gln and Asn. Steric clashes were also detected, by displaying the ligand and protein. The refinement process consists of a restrained minimization of the protein structure by selecting RMSD tolerance. The minimization was restrained to the input protein coordinates by a user-selected RMSD tolerance. For restrained minimization of the co-crystallized protein structure the OPLS-AA force field was used [10]. Glide uses an all-atom force field for accurate energy evaluation.

Receptor grid generation

For performing the docking and scoring of ligands with the receptor, the grid generation is essential for more than one conformation on binding to ensure possible active sites. The grid is generated by the Receptor Grid Generation. The OPLS_2005 force field was used for grid generation, which allows a proper treatment of metals In receptor grid generation, ligand molecule was picked and selects the site tab for determining the position of scoring grids. The grid box or enclosing box contains ligand atoms and have a size less than 50 Å.

Ligand docking and scoring function

All prepared ligands were docked by the use of molecular docking tool, Glide 5.5, scored in "Extra precision" (XP) mode. Glide is designed to search the positional, orientational and conformational space available to the ligands [11]. This has been accomplished by using a series of hierarchical filters. These initial filters use grid-based method to analyze the space fit of the ligand to the defined active site [12], the ligands were flexible and protein was rigid, but the active site of protein has slight flexibility. Finally, all receptor flexible ligands were docked into different receptor grids [13-14]. Initial poses pass through the filters for the initial geometry and complementarity "fit" between the ligand and receptor molecules enter the final step of a process, which associate the evaluation and energy-minimization of a grid approximation to the OPLS-AA nonbonded ligand-receptor interaction energy. So, scoring is associated with energy-minimized poses and finally, energy-minimized poses are again scored by using the GlideScore scoring function. Receptor's shape and properties are represented on a grid by different field sets that allowed more accurate scoring of the ligand pose.

Glide-Score, which is based on ChemScore, predicts the binding affinity and rank-ordering ligands in database screens and contains a steric-clash term and adds buried polar terms.

Glide-Score = 0.065*vdW + Hbond + Lipo + 0.130*Coul + Metal + BuryP + RotB + Site

Where vdW is Van der Waals energy, Hbond is a Hydrogen-bonding, Lipo is a Lipophilicity, Coul represents Coulomb energy, Metal is a Metal-binding, BuryP represents Penalty for buried polar groups, RotB represents Penalty for freezing rotatable bonds, Site represents Polar interactions in the active site.

Pharmacokinetic study

Pharmacokinetic profiles of each designed structure were generated using Qikprop 2.5 (Schrödinger). QikProp predicts physically significant descriptors and pharmaceutically relevant properties of organic compounds. All structure must be three-dimensional and neutralized before using Qikprop. QikProp rapidly analyses atom types and charges, rotor counts, the sample molecule's surface area and volume. QikProp compares a particular molecule's properties with those of 95% of known drugs. QikProp evaluates the "drug-likeness" of the analogs according to Lipinski's rule of five [15-16], which is based on four physicochemical parameter ranges (Molecular weight $\leq$ 500, log P $\leq$ 5, H-bond acceptors $\leq$ 10, H-bond donors $\leq$ 5).

RESULTS AND DISCUSSION

Designing of new chemical entities possessing Isatin nucleus

Many structural investigations suggested that most of NNRTIs have few common structural features that have carboxamide or thiourea moiety as like body which is surrounded by two hydrophobic, substituted aryl moieties as like wings. The structure seems to be a butterfly-like conformation (butterfly with the hydrophilic center and two hydrophobic moieties) that has also been proven by a crystallographic analysis [17] (Fig. 2a).

Analysis of X-ray crystal structure of HIV-RT enzyme suggested that many NNRTIs filled up an allosteric hydrophobic pocket that is a nonnucleoside binding site and bound with the HIV-RT enzyme in a "butterfly-like" manner [18-19]. One wing of this butterfly is made up of π-electron-rich entity in which aryl or allyl substituents are involved by π- π interactions with a hydrophobic pocket which consists of aromatic amino acids (Tyr318, Trp229, Phe227, Tyr181 and Tyr188). The later wing is normally represented by a hetero aromatic ring that bears a functional group which is capable of donating and/or accepting hydrogen bonds with the main chain of the Lys103

and Lys101 (Fig. 2c). The butterfly body of a hydrophobic portion satisfies a small pocket constituted mainly by amino acid side chains of Val179, Val106 and Lys103.

Table 1 Structures of designed Isatin derivatives

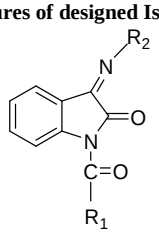

Comp.	R_1	R_2	Comp.	R_1	R_2
S1	-diethyl amine	-morpholine	S26	-dibutyl amine	- pyrimidine
S2	-ethyl methyl amine	-morpholine	S27	-diphenyl amine	- pyrimidine
S3	-dibutyl amine	-morpholine	S28	-ethyl methyl amine	- pyrimidine
S4	-diphenyl amine	-morpholine	S29	-ethyl propyl amine	- pyrimidine
S5	-imidazole	-morpholine	S30	-piperidine	- pyrimidine
S6	-dimethyl amine	-thiazole	S31	-dimethyl amine	-1,2,4- triazole
S7	-diethyl amine	-thiazole	S32	-diethyl amine	-1,2,4- triazole
S8	-ethyl methyl amine	- thiazole	S33	-ethyl methyl amine	-1,2,4- triazole
S9	-methyl propyl amine	- thiazole	S34	-methyl propyl amine	-1,2,4- triazole
S10	-dibutyl amine	- thiazole	S35	-dibutyl amine	-1,2,4- triazole
S11	-piperidine	- thiazole	S36	-diphenyl amine	-1,2,4- triazole
S12	-diphenyl amine	- thiazole	S37	-piperidine	-1,2,4- triazole
S13	-piperazine	- thiazole	S38	-piperazine	-1,2,4- triazole
S14	-pyrrolidine	- thiazole	S39	-pyrrolidine	-1,2,4- triazole
S15	-ethyl propyl amine	- thiazole	S40	-ethyl propyl amine	-1,2,4- triazole
S16	-morpholine	- thiazole	S41	-morpholine	-1,2,4- triazole
S17	-pyrrole	- thiazole	S42	-imidazole	-1,2,4- triazole
S18	-imidazole	- thiazole	S43	-dimethyl amine	-piperidine
S19	-diethyl amine	-piperazine	S44	-methyl propyl amine	- piperidine
S20	-ethyl methyl amine	-piperazine	S45	-dibutyl amine	- piperidine
S21	-dibutyl amine	- piperazine	S46	-diphenyl amine	- piperidine
S22	-diphenyl amine	- piperazine	S47	-piperazine	- piperidine
S23	-pyrrolidine	- piperazine	S48	-dimethyl amine	-pyrazole
S24	-dimethyl amine	- pyrimidine	S49	-diphenyl amine	-pyrazole
S25	-diethyl amine	- pyrimidine	S50	-dibutyl amine	-pyrazole

On the basis of these two observations, diverse derivatives of Isatin were designed. These designed molecules have tried to fit with both these observations in which the iminocarbamoyl moiety (–N=C–CO–N–) constitutes the body and the aryl ring of isatin and the heteroaromatic rings constitute the wings (Sriram *et al*., 2005) (Fig. 2b).

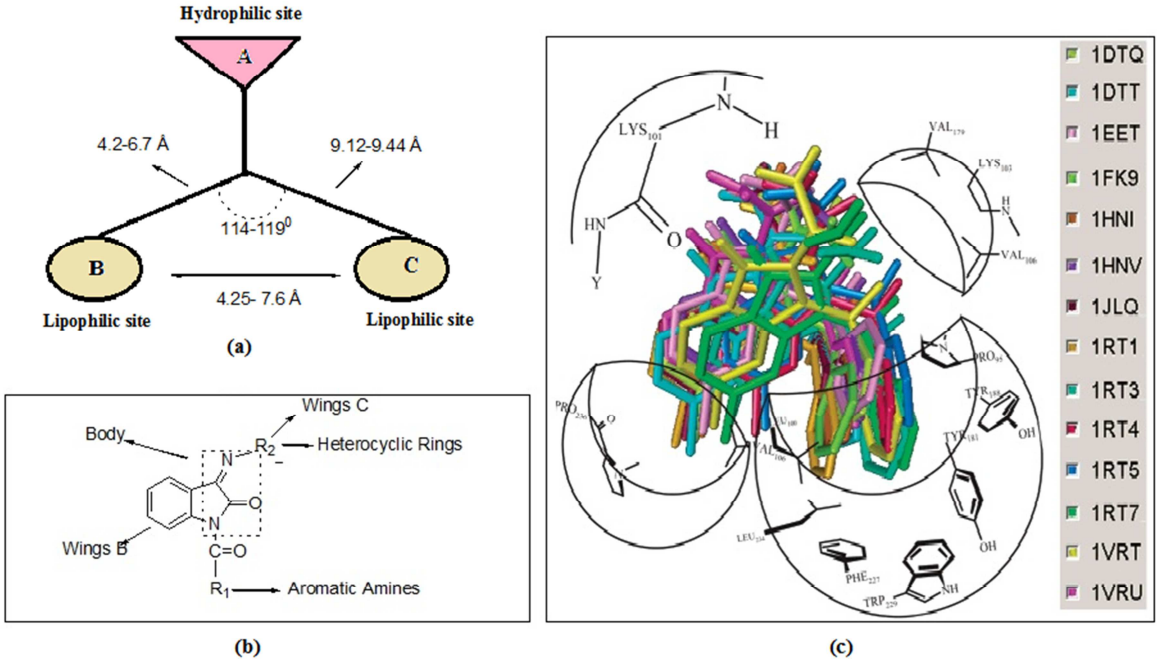

Fig. 2 a Butterfly configuration of NNRTI'S, b Butterfly shape of Isatin derivatives, c Schematic representation of the different NNBSs with ligand bound conformation in the RT complex

Molecular docking study

Molecular docking study was carried out for six PDB structure of the RT enzyme with different substituted Isatin derivatives. The results of the experiment are shown in Table 2.

To visualize the docking results, ligand poses were opened by pose facility option on the table for comparing the best docking poses in the Glide XP Visualizer. Ligand poses were displayed with the receptor along with hydrogen bonds and per-residue interaction information. To predict the bound mode of title compounds, all NNRTIs removes from the active site of the co-crystallized structure individually and again docked into the binding pocket of the PDB structure.

Table 2 Results of docking studies of title compounds

Compounds	Gscore							Ligand activity
	Combined Gsore	1REV	1SV5	1IKY	1KLM	1TKZ	1IKW	
Rilpivirine	-72.58	-13.27	-9.68	-12.77	-10.31	-13.42	-13.13	1TKZ
Etravirine	-63.43	-9.43	-9.87	-10.75	-8.82	-12.17	-12.38	1IKW
S5	-58.6	-11.03	-7.72	-10.05	-10.68	-11.08	-8.03	1TKZ
Efavirenz	-55.96	-9.44	-7.96	-8.75	-9.87	-9.44	-10.48	1IKW
S37	-55.49	-9.15	-8.1	-9.1	-11.38	-8.63	-9.12	1KLM
S30	-54.55	-8.93	-8.74	-9.64	-9.25	-8.8	-9.17	1IKY
S29	-53.45	-8.9	-8.67	-9.84	-9.96	-7.36	-8.7	1KLM
S10	-51.95	-8.47	-7.83	-8.8	-11.14	-7.94	-7.75	1KLM
S22	-51.68	-7.81	-8.58	-9.65	-9.45	-8.25	-7.92	1IKY
S50	-51.58	-9.35	-7.89	-8.03	-10.02	-9.31	-6.97	1KLM
S44	-51.56	-7.58	-7.35	-8.43	-9.94	-9.51	-8.72	1KLM
S4	-51.49	-7.91	-9.5	-9.98	-9.12	-8.02	-6.94	1IKY
S28	-51.14	-8.73	-8.49	-8.35	-9.49	-7.67	-8.39	1KLM
S26	-50.95	-8.31	-8.36	-8.85	-10.2	-6.28	-8.94	1KLM
S39	-50.89	-7.74	-7.87	-10.12	-6.41	-9.97	-8.76	1IKY
S11	-50.66	-7.98	-7.31	-9.59	-9.83	-8.92	-7	1KLM
S3	-50.48	-8.38	-7.64	-8.67	-8.81	-9.35	-7.61	1TKZ
S38	-50	-9.75	-7.17	-8.77	-4.72	-9.81	-9.75	1TKZ
S43	-49.47	-7.91	-8.73	-7.49	-9.27	-9.15	-6.9	1KLM
S42	-49.4	-7.84	-7.35	-8.95	-8.56	-7.56	-9.14	1IKW
S16	-49.39	-8.62	-7.6	-7.85	-9.91	-8.01	-7.37	1KLM
S18	-49.37	-9.18	-7.51	-7.58	-10.48	-7.22	-7.37	1KLM
S12	-49.18	-8.28	-9.27	-9.94	-8.19	-8.19	-5.28	1IKY
S49	-49.04	-8.32	-9.71	-9.61	-8.18	-7.44	-5.76	1SV5
S47	-48.89	-8.33	-7.7	-8.4	-7.37	-8.72	-8.35	1TKZ
S17	-48.83	-7.59	-7.28	-9.08	-10.03	-6.81	-8.02	1KLM
S41	-48.68	-8.55	-7.21	-9.55	-4.92	-8.43	-10	1IKW
S24	-48.01	-8.01	-7.64	-7.89	-9.11	-7.46	-7.87	1KLM
S45	-47.9	-7.42	-7.96	-9.26	-9.53	-8.06	-5.65	1KLM
S46	-47.81	-7.9	-9.99	-10.07	-5.11	-8.7	-6.03	1IKY
S23	-47.54	-8.19	-7.78	-8.34	-7.41	-7.76	-8.05	1IKY
S31	-47.19	-8.39	-7.53	-7.15	-8.58	-7.94	-7.58	1KLM
S6	-46.89	-7.37	-6.41	-7.81	-9.87	-8.14	-7.27	1KLM
S13	-46.77	-7.65	-7.26	-7.84	-8.75	-7.83	-7.41	1KLM
S33	-46.76	-7.65	-6.96	-8.26	-8.28	-7.61	-7.97	1KLM
S48	-46.64	-7.89	-5.93	-7.64	-9.85	-8.09	-7.22	1KLM
S27	-46.62	-7.18	-9.73	-9.66	-5.72	-7.57	-6.73	1SV5
S9	-46.55	-5.76	-7.17	-7.5	-11.7	-6.43	-7.97	1KLM
S19	-46.48	-8	-8	-9.94	-4.79	-7.37	-8.37	1IKY
S35	-46.25	-8.66	-7.9	-7.78	-4.59	-10.47	-6.83	1TKZ
S1	-45.69	-6.62	-5.95	-8.24	-8.68	-9.26	-6.91	1TKZ
S25	-45.61	-7.58	-8.02	-8.15	-8.15	-5.41	-8.27	1IKW
S34	-45.61	-7.82	-6.81	-7.25	-9.06	-7.61	-7.03	1KLM
S15	-45.52	-7.17	-7.2	-7.22	-8.56	-7.33	-8.01	1KLM
S20	-44.21	-8.11	-7.12	-9.64	-4.46	-6.79	-8.07	1IKY
Nevirapine	-43.6	-5.61	-6.73	-8.32	-6.54	-9.33	-7.04	1TKZ
S32	-42.76	-6.75	-6.59	-8.28	-7.72	-7.31	-6.09	1IKY
S7	-42.2	-7.16	-6.88	-7.59	-5.21	-7.7	-7.63	1TKZ
S36	-40.64	-7.52	-7.09	-9.34	-5.05	-7.18	-4.44	1IKY
S8	-39.55	-6.92	-6.68	-7.93	-4.86	-5.88	-7.26	1IKY
S14	-38.23	-7.51	-7.47	-6.51	-4.13	-4.74	-7.85	1IKW
S2	-34.36	-7.88	-6.14	-7.81	-8.75	-9.01	-7.04	1TKZ
Delavirdine	-32.16	-2.23	-7.79	-5.11	-6.1	-4.14	-6.77	1SV5

Ligand-receptor interaction is necessary for successful virtual screening in structure-based drug design. This interaction is best expressed in van der Waals and electrostatic energy terms.

Combined G score (dock score) of compounds S5, S37 and S30 was found to be -58.6, -55.49 and -54.55, respectively, which was comparable with known NNRTIs such as Rilpivirine, Etravirine, Efavirenz, Nevirapine and Delavirdine (combined dock score: -72.58, -63.43, -55.96, -43.6 and -32.16 respectively). On the basis of the combined G score, designed Isatin derivatives have a good binding affinity towards NNBS of RT enzyme.

All known NNRTIs bind in the same manner with the binding pocket of viral enzyme. On the basis of docking results, designed compounds were bound to the binding pockets of the RT enzyme in the same way as NNRTIs bind. Non-nucleoside binding pocket site consists of Five aromatic (Tyr181, Tyr188, Phe227, Trp229 and Tyr318), five hydrophilic (Lys101, Lys102, Lys103, Ser 105, Asp-132) and six hydrophobic (Pro95, Leu100, Val106, Gly190, Leu234, Pro236) amino acids which belongs to p66 subunit and Glu-138 amino acids belonging to the p51 subunit.

Identification of binding pocket site with known NNRTIs predicts the binding conformations with ligands which provide a rationale for designing safe and more efficient compounds. Here, one of the best ligand activity of the compounds for all six crystal structure of protein based on G score is also described. Compound S5 has best ligand activity for 1TKZ protein. The binding conformations of designed isatin derivatives within binding pocket of all six crystal structure of HIV-1 RT were studied which displayed hydrophobic interaction and H-bond interaction with amino acid residues of nonnucleoside binding site site. The protein-ligand steric contact information was also analyzed in the total glide score. This information is best expressed in terms of Van der Waals energy, Coulomb energy and modified Coulomb-Van der Waals interaction energy. H-bond interaction with distance and steric contact information of the protein-ligand complex were depicted in Table 3.

In the binding pocket of RT (1REV), Rilpivirine exhibited two hydrogen bonds with same amino acid Lys101 (1.889 Å and 2.111 Å) (Fig. 3a, e). Amino acid residues involved in hydrophobic interaction were found to be Trp229, Pro236, Asp237, Val189, Leu234 and Pro95. Rilpivirine had Van der Waals energy -46.300 and glide energy -53.968. Whereas compound S5 and S37showed hydrogen bonding with Lys101 (2.214 Å) and Lys103 (2.21 Å), respectively. Hydrophobic interactions were involved with Tyr183, Val189, Trp229, Pro236, Asp237, Leu234 and Pro95 in compound S5 and S37. Compound S5 had Van der Waals energy -48.571 and glide energy -50.097, and S37 showed Van der Waals energy -43.757 and glide energy -46.377. Thus, it can be concluded that designed derivatives like Rilpivirine have similar hydrophobic pocket as like two wings of butterfly-like mode.

Same as in 1SV5 PDB code, Rilpivirine showed hydrophobic interactions with Pro95, Leu100, Val179, Tyr181, Phe227, Tyr318 and hydrogen bonding with His235 (2.06 Å). Compound S5, S37 and S30 had less G score due to absence of hydrogen bonding as compared to Rilpivirine. So, H-bond interactions play a vital role in calculation of glide score. In the binding pocket of RT (1IKY), Efavirenz had a higher G score without H-bond interactions, but had good hydrophobic interactions with Leu100, Val179, Tyr181, Trp229, Pro236 and Tyr318. Compound S30 and S29 showed hydrogen bonding with Asn103 and hydrophobic interactions with Leu100, Val179, Tyr181, Trp229, Pro236 and Tyr318. Compound S32 and S2 have less G score as compared to Efavirenz due to absence of hydrogen bonding interactions and have less hydrophobic interactions.

Similarly, in 1KLM, Etravirine showed two hydrogen bonds with Lys103 (1.85Å) and Leu234 (2.29Å) and have good hydrophobic interactions. Compound S5 and S37 have a higher G score as compared to Etravirine. G score of compound S32 was found less due to bad Van der Waals contacts. The Van der Waals energy of Etravirine was also found higher due H-bonding.

Delaviridine had two hydrogen bonds with Lys101 (1.88 Å and 2.46Å) in the binding pocket of RT (1IKW). It showed hydrophobic interactions with Pro95, Leu100, Val106, Tyr181, Trp229 and Pro236. Compound S30 showed hydrogen bonding with Lys101 (2.39Å) and have less hydrophobic interactions that results less G score as compared to Delaviridine.

In 1TKZ PDB code compound S5 had a higher G score due to the presence of a hydrogen bond with Lys 101 (2.18 Å) and have good hydrophobic interactions (Fig. 3c, d). Nevirapine showed two H-bond interactions with Lys101 (2.44 Å and 2.48 Å) but have less G score due to ugly Van der Waals contacts or less hydrophobic interactions.

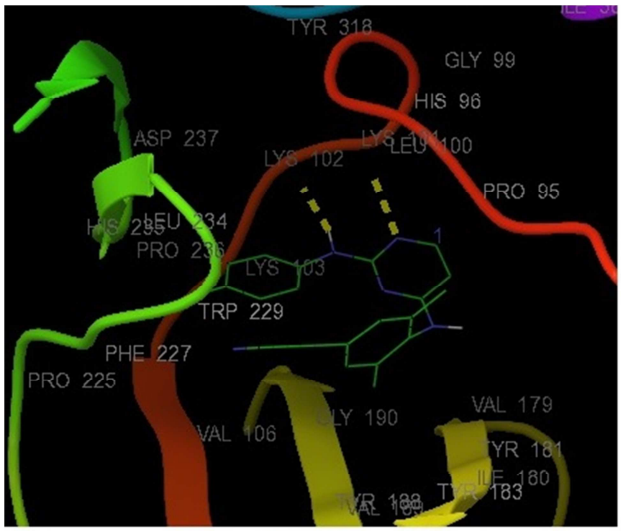

(a)

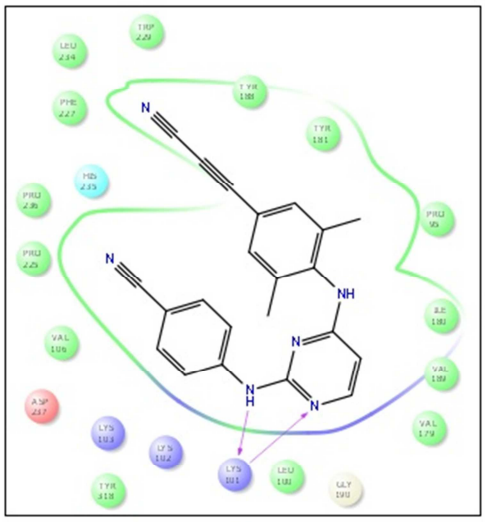

(b)

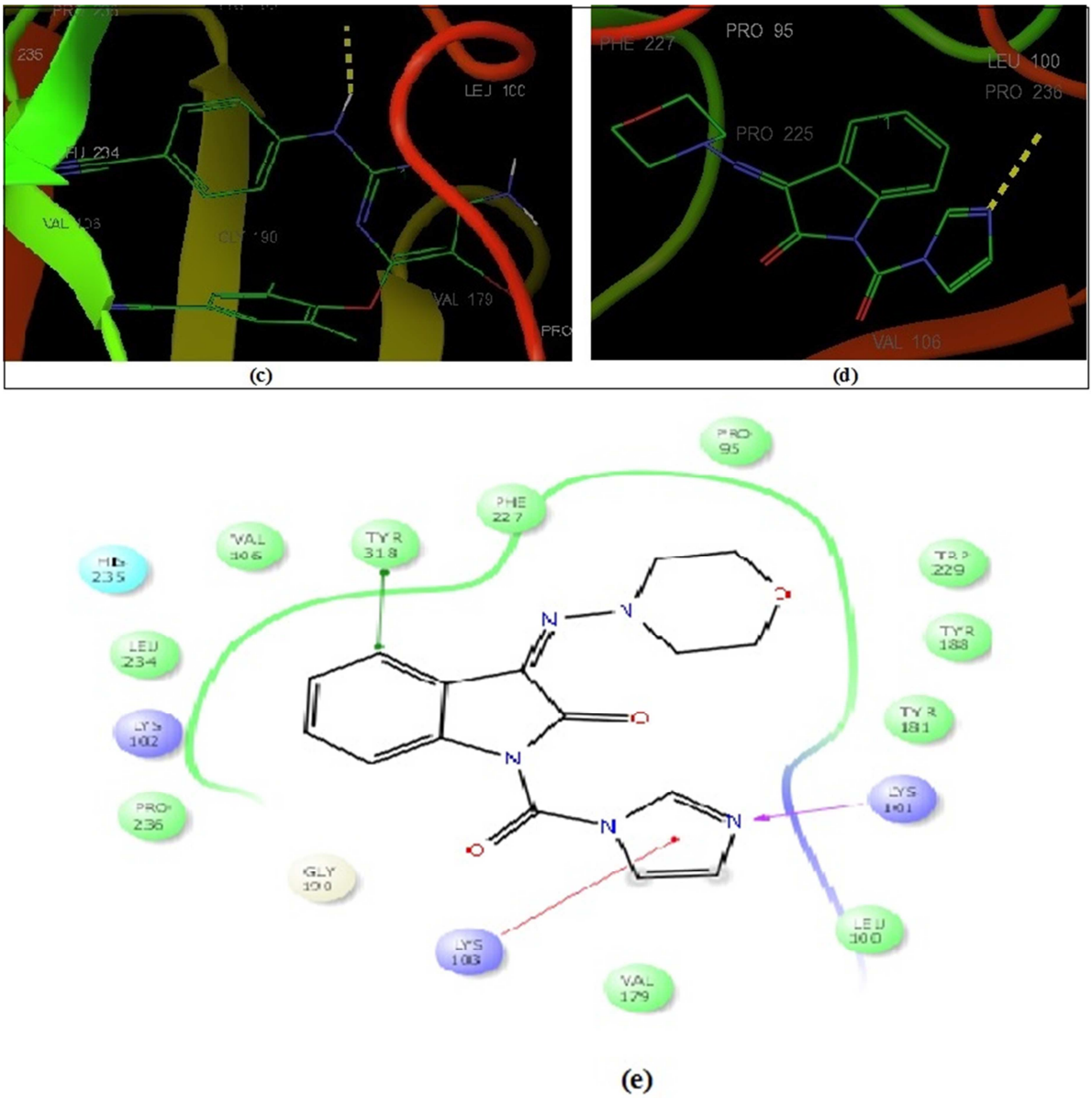

Fig. 3 a Binding view of Rilpivirine in binding pocket of 1REV, b Ligand interaction view of Rilpivirine, c Binding view of Etravirine in binding pocket of 1IKW, d Binding mode of compound S5 in binding pocket of 1TKZ, e Ligand interaction view of compound S5

From ligand interaction diagram of the designed compound, it was found that different residues interact with isatin wing in which some residues contribute to the formation of the binding pocket for the butterfly–like shape of the isatin derivatives. Some residues involved in the π-π stacking (Tyr318), π-cation (Lys103), hydrophobic interactions (Tyr188, Pro95, Leu100, Val106, Tyr181, Trp229 and Pro236) and metal coordination.

After comparing the binding pattern of isatin derivatives in the binding pocket of six different HIV-1 RT proteins with different NNRTIs, it was found that nitrogen containing heterocyclic ring at R_1 position binds in similar patterns and give more active compound. 1,2,4-triazole substitution at R_2 position in Isatin derivatives binds similarly as like Efavirenz. A close comparison suggests that the presence of heterocyclic ring at R_2 position and presence of tertiary nitrogen containing substitution at R_1 position generate more active compound.

Pharmacokinetic study

Both physicochemical descriptors and pharmacokinetically relevant properties of designed compounds were analyzed using QikProp. Here, we reported some descriptors which are essential for prediction of drug-likeness of the compounds. Following descriptors were reported-

1. Molecular weight (mol_MW) (130.0 – 725.0)
2. Predicted octanol/water partition coefficient (Log Po/w) (–2.0 – 6.5)
3. Predicted aqueous solubility, (QPlogS) (–6.5 – 0.5)

4. Predicted apparent MDCK cell permeability (QPPMDCK) in nm/sec (<25 poor, >500 great)
5. Predicted brain/blood partition coefficient, (QPlogBB) (–3.0 – 1.2)
6. Predicted Percent Human Oral Absorption (>80% is high, <25% is poor)

Table 3 Hydrogen bond interactions of Isatin derivatives with amino acid residues along with van der waals energy

PDB code	Compounds	G score	H-bond interaction	Distance	glide evdw	glide energy
1REV	S5	-11.03	NH-Lys101	2.21	-48.571	-50.097
	S37	-9.15	NH-Lys103	2.21	-43.757	-46.377
	S30	-8.93	-	-	-36.368	-37.597
	S29	-8.9	-	-	-38.583	- 39.552
	S32	-6.75	NH-Lys101	2.22	-35.587	-38.084
	S2	-7.88	NH-Lys101	2.06	-37.624	-42.816
	Rilpivirine	-13.27	NH-Lys101	2.11		
			NH-Lys101	1.89	-46.300	-53.968
	Etravirine	-9.43	NH-Lys101	2.05	-45.413	-48.559
	Efavirenz	-9.44	NH-Lys101	1.88	-35.234	-36.568
	Nevirapine	-5.61	-	-	-40.330	-41.624
	Delavirdine	-2.23	NH-Gly93	2.11	-35.782	-40.064
1SV5	S5	-7.72	-	-	-31.958	-32.805
	S37	-8.1	-	-	-28.389	-29.312
	S30	-8.74	-	-	-30.519	-30.979
	S29	-8.67	-	-	-40.826	-41.986
	S32	-6.59	-	-	-34.995	-37.534
	S2	-6.14	-	-	-31.641	-35.33
	Rilpivirine	-9.68	NH-His235	2.06	-46.101	-48.890
	Etravirine	-9.87	NH-Lys102	2.29		
			NH-Tyr318	2.04	-39.550	-44.176
	Efavirenz	-7.96	-	-	-34.518	-36.815
	Nevirapine	-6.73	-	-	-34.840	-36.877
	Delavirdine	-7.79	-	-	-51.89	-54.610
1IKY	S5	-10.05	NH-Lys101	1.91	-34.895	-38.909
	S37	-9.1	-	-	-42.490	-42.187
	S30	-9.64	NH-Asn103	1.97	-40.396	-41.954
	S29	-9.84	NH-Asn103	2.03	-33.641	-35.283
	S32	-8.28	-	-	-39.437	-39.292
	S2	-7.81	-	-	-30.525	-30.935
	Rilpivirine	-12.77	NH-Lys101	1.84	-51.451	-55.915
	Etravirine	-10.75	NH-Lys101	1.83	-49.448	-54.516
	Efavirenz	-8.75	-	-	-34.669	-35.938
	Nevirapine	-8.32	NH-Lys101	2.36	-31.797	-34.576
	Delavirdine	-5.11	-	-	-40.332	-42.222
1KLM	S5	-10.68	NH-Lys101	2.06	-36.200	-38.268
	S37	-11.38	NH-Lys103	2.08	-30.803	-33.141
	S30	-9.25	-	-	-47.968	-47.549
	S29	-9.96	-	-	-46.004	-45.265
	S32	-7.72	-	-	-32.413	-34.833
	S2	-8.75	-	-	-35.103	-36.056
	Rilpivirine	-10.31	NH-Leu234	1.97	-47.061	-52.312
	Etravirine	-8.82	NH-Lys103	1.85	-47.724	-52.526
			NH-Leu234	2.29		
	Efavirenz	-9.87	NH-Lys101	1.64	-30.006	-32.780
	Nevirapine	-6.54	-	-	-30.131	-31.151
	Delavirdine	-6.1	NH-Lys103	1.76		
			OH-Lys103	1.9	-56.615	-67.453
1IKW	S5	-8.03	-	-	-31.943	-33.047
	S37	-9.12	-	-	-37.848	-39.057
	S30	-9.17	NH-Lys101	2.39	-39.163	-42.675
	S29	-8.7	-	-	-35.965	-36.379
	S32	-6.09	NH-Lys101	2.4	-40.046	-42.408
	S2	-7.04	-	-	-31.027	-32.804
	Rilpivirine	-13.13	NH-Lys101	2.17		
			NH-Lys101	1.62	-24.328	-32.479
	Etravirine	-12.38	NH-Lys101	1.67	-36.573	-43.127
	Efavirenz	-10.48	NH-Lys101	2.03	-35.894	-37.548
	Nevirapine	-7.04	-	-	-27.392	-28.031
	Delavirdine	-6.77	NH-Lys101	1.88		
			OH-Lys101	2.46	-38.168	-41.409
1TKZ	S5	-11.08	NH-Lys101	2.18	-46.304	-50.179
	S37	-8.63	-	-	-32.910	-34.592
	S30	-8.8	-	-	-49.229	-51.589
	S29	-7.36	-	-	-33.761	-34.087
	S32	-7.31	NH-Lys101	2.07	-39.765	-42.947
	S2	-9.01	OH-Lys101	1.89	-37.946	-42.896
	Rilpivirine	-13.42	NH-Lys101	1.56		
			NH-Lys101	2.1	-38.293	-45.586
	Etravirine	-12.17	NH-Lys101	2.11		
			NH-His235	2.25	-36.247	-35.405
	Efavirenz	-9.44	NH-Lys101	2.03	-34.231	-35.166
	Nevirapine	-9.33	NH-Lys101	2.44		
			OH-Lys101	2.48	-41.088	-45.141
	Delavirdine	-4.14	NH-Lys101	2.1	-32.863	-38.790

All designed compounds showed significant values which were analyzed for the descriptors. The pharmacokinetic profiles of designed compounds are reported in Table 4. Here, only three properties are shown which were analyzed for Lipinski's rule of five, and aqueous solubility greater than -7. All the compounds were found to have zero Lipinski violation and have the most appropriate Log Po/w value for better biological efficacy.

Aqueous solubility (QPlogS) may be expressed as the equilibrium concentration of the solute in a saturated solution in the crystalline solid and measured in mol dm^{-3}.

Brain/blood partition coefficient (QPlogBB) parameter predicts the ability of the compounds to pass the blood-brain barrier which is essential for designing an anti-HIV drug. Apparent MDCK cell permeability (QPPMDCK) parameter predicts the MDCK (Madin-Darby canine kidney) cell permeability. MDCK cells are an important tool for rapid membrane permeability screening [20], and also a good mimic for the blood-brain barrier. Percent human oral absorption was also evaluated for designed compounds.

Table 4 Results of pharmacokinetic study of designed Isatin derivatives using QikProp

Compounds	mol_MW	QPlogPo/w	QPlogS	QPlogBB	QPPMDCK	Percent Human Oral Absorption	Rule of Five
S1	330.386	1.468	-1.838	-0.288	1180.261	92.527	0
S2	316.359	1.086	-1.448	-0.26	1079.378	88.983	0
S3	386.493	3.003	-3.23	-0.421	1744.432	100	0
S4	426.474	3.279	-3.547	-0.244	1415.588	100	0
S5	325.326	0.244	-0.654	-0.431	594.955	79.371	0
S6	300.334	1.301	-2.118	-0.479	663.058	84.046	0
S7	328.388	1.964	-2.532	-0.582	706.865	88.317	0
S8	314.361	1.682	-2.574	-0.514	746.475	87.632	0
S9	328.388	2.304	-2.898	-0.304	1762.525	94.931	0
S10	384.495	3.798	-4.533	-0.581	1916.162	100	0
S11	340.399	2.255	-3.182	-0.229	1487.545	93.888	0
S12	424.476	3.807	-4.447	-0.5	980.841	100	0
S13	341.387	0.647	-1.938	-0.702	39.747	58.593	0
S14	326.372	1.757	-2.833	-0.598	536.979	85.03	0
S15	342.415	2.434	-3.168	-0.57	951.359	93.62	0
S16	342.372	1.196	-1.879	-0.225	1458.875	87.213	0
S17	322.341	1.847	-2.488	-0.363	1094.908	88.389	0
S18	323.328	0.538	-1.424	-0.872	251.937	72.142	0
S19	329.401	1.374	-1.616	0.075	258.864	80.389	0
S20	315.374	1.072	-1.602	0.024	209.5	76.434	0
S21	381.477	2.51	-2.338	-0.237	243.958	86.046	0
S22	425.489	2.982	-3.301	-0.082	195.469	87.672	0
S23	327.385	0.993	-1.996	-0.171	114.498	71.591	0
S24	295.3	0.778	-1.441	-0.583	392.192	80.06	0
S25	323.354	1.269	-1.834	-0.706	437.22	83.6	0
S26	379.461	3.053	-3.662	-1.038	444.125	94.159	0
S27	419.442	3.236	-4.079	-0.822	377.364	94.64	0
S28	309.327	0.96	-1.499	-0.658	397.542	81.13	0
S29	337.38	1.76	-2.032	-0.719	448.33	86.798	0
S30	335.365	1.581	-2.617	-0.608	418.534	85.446	0
S31	284.277	0.331	-0.892	-0.511	472.407	78.777	0
S32	312.33	0.766	-1.42	-0.929	227.156	76.018	0
S33	298.304	0.641	-1.159	-0.641	397.88	79.239	0
S34	312.33	0.881	-1.441	-0.727	390.243	80.814	0
S35	368.438	2.08	-2.752	-1.332	184.019	82.804	0
S36	408.418	2.959	-3.501	-0.556	717.339	100	0
S37	324.341	0.874	-2.008	-0.786	261.484	77.93	0
S38	325.329	-0.397	-1.027	-0.767	24.051	52.531	0
S39	310.315	0.432	-1.578	-0.947	171.239	71.945	0
S40	324.341	1.305	-1.798	-0.837	360.738	82.456	0
S41	326.314	-0.198	-0.503	-0.666	307.385	72.676	0
S42	307.271	-0.609	-0.19	-1.087	108.219	62.185	0
S43	300.36	1.818	-2.537	-0.241	994.161	92.804	0
S44	328.413	2.61	-3.166	-0.252	1378.342	100	0
S45	384.52	4.177	-5.023	-0.546	1452.082	100	0
S46	424.501	4.445	-5.205	-0.244	1556.181	100	0
S47	341.412	1.275	-2.267	-0.103	133.312	74.621	0
S48	283.289	1.065	-1.792	-0.584	399.276	81.856	0
S49	407.431	3.621	-4.235	-0.626	575.58	100	0
S50	367.45	3.34	-4.081	-0.931	576.608	100	0
Delavirdine	427.77	3.388	-6.728	-1.396	439	84	0
Nevirapine	266.302	2.36	-3.208	-0.07	1082.042	100	0
Efavirenz	315.679	3.582	-4.911	0.131	7631.099	100	0
Rilpivirine	364.409	3.434	-6.573	-1.547	122.958	90.735	0
Etravirine	435.282	2.334	-5.855	-2.244	29.602	70.52	0

CONCLUSION

Molecular docking is the one of the most promising approaches in structure based drug-design. This computational technique provides the information about the binding affinity and conformation of ligand with a protein by forming protein-ligand conformation. The molecular docking results suggested that designed Isatin derivatives bind to the

RT enzyme in a same manner as known NNRTIs. Pharmacokinetic studies concluded that the designed compounds have good ADME properties as well as the drug-likeness. Compounds S5, S37 and S30 have better G score as compared to standards and have a good pharmacokinetic profile with drug-like properties. So, these compounds may be considered for further studies, *i.e.* synthesis, pharmacological screening, QSAR etc. This study will provide the platform for designing new compounds with potential anti-HIV activity.

REFERENCES

[1] De Clercq E (**2002**) Strategies in the design of antiviral drugs. *Nat Re Drug Discov* 1:13-25
[2] Balzarini J (**2004**) Current status of nonnucleoside reverse transcriptase inhibitors of human immuno deficiency virus type 1. *Curr Top Med Chem* 4:921–944
[3] Pandeya SN, Sriram D, Nath G, De Clercq E (**2000**) Synthesis, antibacterial, antifungal and anti-HIV activities of norfloxacin Mannich bases. *Eur J Med Chem* 35(2):249–255
[4] Sarangapani MR, Reddy VM (**1994**) Pharmacological evaluation of 1-(N,N-disubstituted aminomethyl)-3-imino-(2-phenyl-3,4-dihydro-4-oxo-quinazolin-3-yl) indolin-2-ones. *Indian J Pharm Sci* 56:174–177
[5] Daisley RW, Shah VK (**1984**) Synthesis and antibacterial activity of some 5-nitro-2(3H)-one and their N-Mannich bases. *J Pharm Sci* 73:407–409
[6] Varma RS, Nobles WL (**1967**) Synthesis and antiviral and antibacterial activity of certain N dialkylaminomethyl isatin b thiosemicarbazone. *J Med Chem* 10:972–974
[7] Singh SP, Shukla SK, Awasthi LP (**1983**) Synthesis of some 3-(40-nitrobenzoylhydrazone)-2-indolinones as potential antiviral agents. *Curr Sci* 52(16):766–769
[8] Palluotto F, Carotti A, Casini G, Campagna F, Genchi G, Rizzo M, De Sarro (**1996**) Structure-activity relationships of 2-aryl-2, 5-dihydropyridazino [4, 3-b] indol-3 (3H)-ones at the benzodiazepine receptor. *Bioorg & med chem* 4(12):2091-2104.
[9] Hayes MJ, Stein M, Weiser J (**2004**) Accurate calculations of ligand binding free energies. *J Phys Chem* 108:3572–3580
[10] Jorgensen WL, Maxwell DS, Tirado-Rives J (**1996**) Development and testing of the OPLS all-atom force field on conformational energetics of organic liquids. *J Am Chem Soc* 118:11225–11236
[11] Friesner RA, Banks JL, Murphy RB, Halgren TA, Klicic JJ, Mainz DT, Repasky MP, Knoll EH (**2004**) Glide: a new approach for rapid, accurate docking and scoring: 1. Method and assessment of docking accuracy. *J Med Chem* 47:1739–1749
[12] Pawar V S, Lokwani D K, Bhandari S V, Bothara K G, Chitre T S, Devale T L, Modhave N S, Parikh J K (**2011**) Design, docking study and ADME prediction of Isatin derivatives as anti-HIV agents. *Med Chem Res* 20:370-380
[13] Carlson HA, Masukawa KM, McCammon JA (**1999**) Method for including the dynamic fluctuations of a protein in computer aided drug design. *J Phys Chem* 103:10213–10219
[14] Carlson HA, Masukawa KM, Rubins K, Bushman FD, Jorgensen WL, Lins RD, Briggs JM, McCammon JA (**2000**) Developing a dynamic pharmacophore model for HIV-1 integrase. *J Med Chem* 43:2100–2114
[15] Lipinski C A (**2004**) Lead-and drug-like compounds: the rule-of-five revolution. *Drug Discov Today*: *Techn* 1:337-341.
[16] Lipinski CA, Lombardo F, Dominy BW, Feeney PJ (**2001**) Experimental and computational approaches to estimate solubility and permeability in drug discovery and development settings. *Adv Drug Deliv Rev* 46:3–26
[17] Sriram D, Bal TR, Yogeeswari P (**2005**) Newer aminopyrimidinimino isatin analogues as non-nucleoside HIV-1 reverse transcriptase inhibitors for HIV and other opportunistic infections of AIDS, design, synthesis and biological evaluation. *Farmaco* 60:377–384
[18] Ragno R, Frasca S, Manetti F, Brizzi A, Massa S (**2005**) HIV-reverse transcriptase inhibition: inclusion of ligand-induced fit by cross dockingstudies. *J Med Chem* 48:200–212
[19] Schiifer W, Friebe W, Leinert H, Mertens A, Poll T, Saal W, Zilch H, Nuber B, Zieglertsf ML (**1993**) Non-nucleoside inhibitors of HIV-f reverse transcriptase: molecular modeling and X-ray structure investigations. *J Med Chem* 36:726–732
[20] Irvine J D, Takahashi L, Lockhart K, Cheong J, Tolan J W, Selick H E, Grove J R (**1999**) MDCK (Madin–Darby canine kidney) cells: a tool for membrane permeability screening. *J Pharm Sci* 88:28-33.